Structural Engineering and Mechanics, *Vol. 54, No. 4 (2015) 809-827*
DOI: http://dx.doi.org/10.12989/sem.2015.54.4.809

Evaluation of energy response of space steel frames subjected to seismic loads

Kadir Ozakgul*

Department of Civil Engineering, Istanbul Technical University, Maslak 34469, Istanbul, Turkey

(Received September 12, 2014, Revised January 16, 2015, Accepted April 4, 2015)

Abstract. In this paper, seismic energy response of inelastic steel structures under earthquake excitations is investigated. For this purpose, a numerical procedure based on nonlinear dynamic analysis is developed by considering material, geometric and connection nonlinearities. Material nonlinearity is modeled by the inversion of Ramberg-Osgood equation. Nonlinearity caused by the interaction between the axial force and bending moment is also defined considering stability functions, while the geometric nonlinearity caused by axial forces is described using geometric stiffness matrix. Cyclic behaviour of steel connections is taken into account by employing independent hardening model. Dynamic equation of motion is solved by Newmark's constant acceleration method in the time history domain. Energy response analysis of space frames is performed by using this proposed numerical method. Finally, for the first time, the distribution of the different energy types versus time at the duration of the earthquake ground motion is obtained where in addition error analysis for the numerical solutions is carried out and plotted depending on the relative error calculated as a function of energy balance versus time.

Keywords: seismic energy response; inelastic steel structure; earthquake ground motion; Ramberg-Osgood equation; independent hardening model; stability functions

1. Introduction

Seismic response of structures subjected to earthquake ground motion may be characterized in terms of distribution of seismic input energy imparted to the structure and its various energy components versus time. The seismic input energy of a system consists of kinetic energy, viscous damping energy, irrecoverable hysteretic energy and recoverable elastic strain energy (Zahrah and Hall 1984, Uang and Bertero 1990). Seismic energy evaluation in structures has been studied by many researchers (Leger and Dussault 1992, Salazar and Haldar 2001, Wong and Yang 2002, Segal and Val 2006, Wong and Zhao 2007, Kalkan and Kunnath 2008, Wang and Wong 2009). Energy-based approach for seismic resistant design and seismic damage assessment of structures has also been carried out by a number of researchers (Manfredi 2001, Wong and Wang 2001, Moustafa 2011, Gong *et al.* 2012). Actual quantification of seismic energy for a structure subjected to seismic loading depends on the accuracy of its inelastic behaviour, thus in many previous studies, the nonlinear behavior of steel structures has been experimentally and

*Corresponding author, Ph.D., E-mail: ozakgulk@itu.edu.tr

http://www.techno-press.org/?journal=sem&subpage=8 ISSN: 1225-4568 (Print), 1598-6217 (Online)

analytically investigated.

Conventional analysis for steel frame structures are based on the assumption that the beam-to-column connections are either fully rigid or ideally pinned. However, in reality all types of connections are flexible or semi-rigid where the behaviour lies between fully restrained and partially restrained. Therefore, numerical models developed with flexible connections can better represent the real structural behaviour in the analysis of frames. Nonlinear analysis for steel frames with rigid and semi-rigid connections has been performed and numerical models based on the nonlinear behaviour have been proposed and published by many researchers (Liew *et al.* 2000, Shugyo 2003, Chiorean and Barsan 2005, Ngo-Huu *et al.* 2007, Chiorean 2009, Thai and Kim 2011, Ngo-Huu *et al.* 2012, Nguyen and Kim 2013). In these studies, nonlinear material behavior of structures has been considered using plastic hinge concept based on the lumped plasticity assumption or fiber plastic hinge concept where the cross-section is partitioned into fibers, so that the plastification at each fiber can be tracked with uniaxial stress-strain relationship. Geometrical nonlinear effects have been generally considered using stability stiffness functions for each member of steel frame. Nonlinear behaviour of connections has been described by using various nonlinear mathematical models representing moment-rotation relationship where flexible connections have been simulated by rotational springs at the ends of the beam members.

The purpose of this study is to examine energy responses of inelastic steel structures subjected to various seismic loadings. Nonlinear behavior of these structures is described by using an algorithm based on material, geometry and connection nonlinearities. Material nonlinearity is considered by using plastic hinge approach based on the zero length plastic hinge placed at the member ends where the nonlinear force-deformation relation is defined by using the inverse of Ramberg-Osgood function. Geometric nonlinearity including P-Δ and P-δ effects is considered by geometric stiffness matrix and stability functions, respectively. To describe the nonlinear behavior of connections under earthquake excitation, independent hardening model is used. The results obtained from the proposed analysis are compared with the corresponding values calculated using a commercial finite element analysis software SAP2000 (2011) in terms of accuracy and computational time. Then, energy response analysis based on seismic energy formulations is carried out. Time-history response for each energy type such as input energy, damping energy, dissipated energy, strain energy and kinetic energy is obtained. Finally, error analysis of the proposed numerical method is achieved by using energy equilibrium concept.

2. Formulation of beam-column element

2.1 Elasto-plastic tangent stiffness matrix

Nonlinear moment-rotation (M-θ) and axial force-deformation (P-ΔL) behaviors formed at the ends of the space members are modeled by the inverse of Ramberg-Osgood function, as given in Eqs. (1) and (2) (Jonatowski and Birnstiel 1970, Uzgider 1980). Positive direction of end forces and displacements for a space frame member is shown in Fig. 1. Moreover, hysteresis loops consisting of skeleton and branch curves are also defined, as space frames considered are dynamically loaded. Since the tangent stiffness of the nonlinear 3D frames is determined by using a step-by step solution procedure, the member force-deformation relationships are expressed in an incremental form.

$$M_i = \frac{K_i \cdot \theta_i}{\left[1 + \left|\frac{K_i \cdot \theta_i}{M_{ip}}\right|^n\right]^{1/n}}, \; i = x, y \tag{1}$$

$$P = \frac{K_p \cdot \Delta L}{\left[1 + \left|\frac{K_p \cdot \Delta L}{P_y}\right|^n\right]^{1/n}} \tag{2}$$

where K_i and K_p are the elastic member bending and axial stiffness, respectively; M and θ are the moment and rotation; N and ΔL are the axial force and axial deformation; M_p is the plastic moment capacity while P_y is the plastic axial force capacity (squash load), and n is a constant defining the shape of the stress-strain relationship.

The incremental force-displacement equation may be written for a 3D elasto-plastic beam-column element as

$$\begin{Bmatrix} \Delta P \\ \Delta T \\ \Delta M_{xi} \\ \Delta M_{xj} \\ \Delta M_{yi} \\ \Delta M_{yj} \end{Bmatrix} = \begin{bmatrix} \frac{EA}{L}\Big/g & 0 & 0 & 0 & 0 & 0 \\ 0 & \frac{GJ}{L} & 0 & 0 & 0 & 0 \\ 0 & 0 & S_1\frac{4EI_x}{L}\Big/r & S_2\frac{2EI_x}{L}(r+s)\Big/2rs & 0 & 0 \\ 0 & 0 & S_2\frac{2EI_x}{L}(r+s)\Big/2rs & S_3\frac{4EI_x}{L}\Big/s & 0 & 0 \\ 0 & 0 & 0 & 0 & S_4\frac{4EI_y}{L}\Big/h & S_5\frac{2EI_y}{L}(h+d)\Big/2hd \\ 0 & 0 & 0 & 0 & S_5\frac{2EI_y}{L}(h+d)\Big/2hd & S_6\frac{4EI_y}{L}\Big/d \end{bmatrix} \cdot \begin{Bmatrix} \Delta(\Delta L) \\ \Delta\theta_T \\ \Delta\phi_{xi} \\ \Delta\phi_{xj} \\ \Delta\phi_{yi} \\ \Delta\phi_{yj} \end{Bmatrix} \tag{3}$$

where M and ϕ are the bending moment and corresponding rotation; P and ΔL are the axial force and axial deformation; T and θ_T are the torsional moment and torsional rotation; A, I_x, I_y and L are the cross-section area, the moment of inertia with respect to x and y axis of the section and the length of the beam-column element; E, G and J are the elastic modulus, shear modulus and torsional constant of the material used, respectively; g, d, h, r and s are the elasto-plastic correction factors (Jonatowski and Birnstiel 1970, Uzgider 1980); S_1, S_2, S_3, S_4, S_5 and S_6 are stability functions (Ekhande *et al.* 1989).

Material nonlinearity is modeled by using the concentrated plastic hinge approach. It is assumed that plastic hinge occurrences between the member ends are not allowed, and a plastic hinge having a zero-length form occurs whenever internal forces satisfy the plasticity criterion expressed by a force-space interaction function. This plastic interaction function is described by Orbison plastic interaction surface (Orbison *et al.* 1982) as follows

$$1.15p^2 + m_x^2 + m_y^4 + 3.67p^2 m_x^2 + 3.00p^6 m_y^2 + 4.65m_x^4 m_y^2 = 1.0 \tag{4}$$

in which, $p=P/P_y$ is the ratio of the axial force to the squash load; $m_x=M_x/M_{xp}$ and $m_y=M_y/M_{yp}$ are

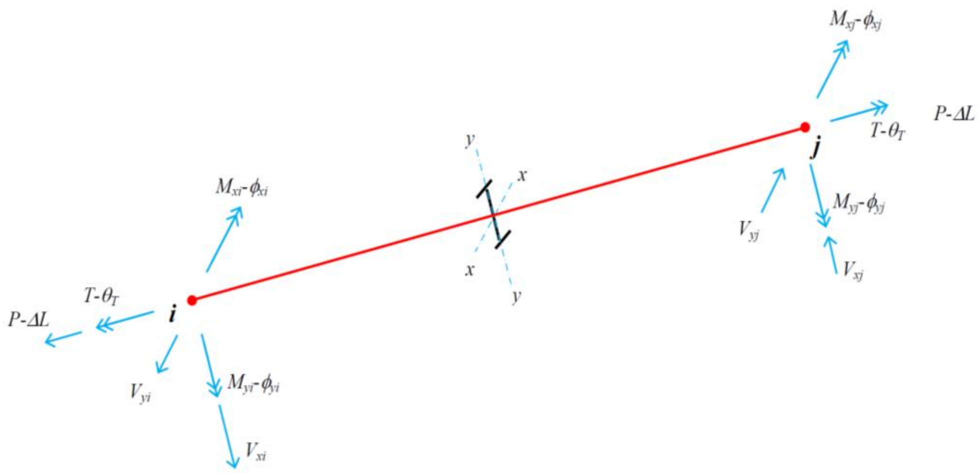

Fig. 1 End forces and displacements of a space frame member

the ratio of the bending moment to the corresponding plastic moment for the strong and weak axises, respectively.

Normalized parameters corresponding to a force vector acting on a given cross-section define a point in the force space or equivalently, a vector from the origin of the space to this point. If the normalized force vector does not reach the yield surface, the cross-section is assumed to remain fully elastic with having no stiffness reduction and no occurence of a plastic flow. Whenever the vector reaches the surface, every fiber in the cross-section is assumed to be stressed to the yield point so that an unrestricted plastic flow will occur. Then, the element stiffness is reduced to consider the effect of plastification at the member ends. If this force vector exceeds the yield surface i.e. yield condition, then the member internal forces need to be corrected where this vector is forced to return to the yield surface without changing its direction.

2.2 Geometric nonlinearity

Geometric nonlinearity (P-Δ) caused by axial force in a frame is described by using the geometric stiffness matrix. The nonlinearity (P-δ) caused by the interaction between the axial force and bending moment in a member is also defined by stability functions (Chen and Chan 1995, Chan and Zhou 1995, Kim *et al.* 2001, White *et al.* 2006).

2.2.1 Stability functions accounting for second order effects

Stability functions are used to consider the second-order effects since they can account for the stiffness degradation caused by the interaction between the axial force and bending moments. The stability functions presented in Eq. (3) are defined as follows

$$S_1 = S_3 = \begin{cases} \dfrac{1}{4} \cdot \dfrac{(\alpha L) \cdot Sin(\alpha L) - (\alpha L)^2 \cdot Cos(\alpha L)}{2 - 2 \cdot Cos(\alpha L) - (\alpha L) \cdot Sin(\alpha L)} & if \;\; P < 0 \\[2ex] \dfrac{1}{4} \cdot \dfrac{(\alpha L)^2 \cdot Cosh(\alpha L) - (\alpha L) \cdot Sinh(\alpha L)}{2 - 2 \cdot Cosh(\alpha L) + (\alpha L) \cdot Sinh(\alpha L)} & if \;\; P > 0 \end{cases} \tag{5}$$

$$S_2 = \begin{cases} \dfrac{1}{2}\cdot\dfrac{(\alpha L)^2 - (\alpha L)\cdot Sin(\alpha L)}{2-2\cdot Cos(\alpha L) - (\alpha L)\cdot Sin(\alpha L)} & if\ \ P<0 \\ \dfrac{1}{2}\cdot\dfrac{(\alpha L)\cdot Sinh(\alpha L) - (\alpha L)^2}{2-2\cdot Cosh(\alpha L) + (\alpha L)\cdot Sinh(\alpha L)} & if\ \ P>0 \end{cases} \tag{6}$$

$$S_4 = S_6 = \begin{cases} \dfrac{1}{4}\cdot\dfrac{(\beta L)\cdot Sin(\beta L) - (\beta L)^2\cdot Cos(\beta L)}{2-2\cdot Cos(\beta L) - (\beta L)\cdot Sin(\beta L)} & if\ \ P<0 \\ \dfrac{1}{4}\cdot\dfrac{(\beta L)^2\cdot Cosh(\beta L) - (\beta L)\cdot Sinh(\beta L)}{2-2\cdot Cosh(\beta L) + (\beta L)\cdot Sinh(\beta L)} & if\ \ P>0 \end{cases} \tag{7}$$

$$S_5 = \begin{cases} \dfrac{1}{2}\cdot\dfrac{(\beta L)^2 - (\beta L)\cdot Sin(\beta L)}{2-2\cdot Cos(\beta L) - (\beta L)\cdot Sin(\beta L)} & if\ \ P<0 \\ \dfrac{1}{2}\cdot\dfrac{(\beta L)\cdot Sinh(\beta L) - (\beta L)^2}{2-2\cdot Cosh(\beta L) + (\beta L)\cdot Sinh(\beta L)} & if\ \ P>0 \end{cases} \tag{8}$$

where $\alpha^2=P/EI_x$, $\beta^2=P/EI_y$ and P is positive for tension.

2.2.2 Geometric stiffness matrix

The element geometric stiffness matrix is composed of changes in nodal forces due to second order effects (P-Δ) of axial nodal forces in case of rigid body rotation of a frame member. If a member is permitted to sway, additional shear forces will occur in the member (Kim *et al.* 2001). These additional forces caused by the member end displacements can be expressed as,

$$\{f_g\} = [S_g]\ \{x\} \tag{9}$$

where $\{f_g\}$, $\{x\}$ and $[S_g]_{12\times12}$ are additional end force vector, end displacement vector, and element geometric stiffness matrix, respectively.

They may be written as

$$f_g^T = \{f_{g1}\ \ f_{g2}\ \ f_{g3}\ \ f_{g4}\ \ f_{g5}\ \ f_{g6}\ \ f_{g7}\ \ f_{g8}\ \ f_{g9}\ \ f_{g10}\ \ f_{g11}\ \ f_{g12}\} \tag{10}$$

$$x^T = \{x_1\ \ x_2\ \ x_3\ \ x_4\ \ x_5\ \ x_6\ \ x_7\ \ x_8\ \ x_9\ \ x_{10}\ \ x_{11}\ \ x_{12}\} \tag{11}$$

$$[S_g]_{12x12} = \begin{bmatrix} [S_0]_{6x6} & [S_0]_{6x6} \\ [S_0]_{6x6} & [S_c]_{6x6} \end{bmatrix} \tag{12}$$

where, $[S_0]_{6\times6}$ is a zero matrix and

$$[S_c]_{6x6} = \begin{bmatrix} -P/L & 0 & 0 & P/L & 0 & 0 \\ 0 & 0 & 0 & 0 & 0 & 0 \\ 0 & 0 & -P/L & 0 & 0 & P/L \\ P/L & 0 & 0 & -P/L & 0 & 0 \\ 0 & 0 & 0 & 0 & 0 & 0 \\ 0 & 0 & P/L & 0 & 0 & -P/L \end{bmatrix} \tag{13}$$

2.3 Semi-rigid connection modelling

Generally, forces transmitted by the beam-column connections consist of axial force, shear force, bending moment and torsion. However, as axial, shear or torsional deformations are rather small compared with the rotational deformation of connections, their effects are negligible. So the deformation behavior of a connection can be described by a moment-rotation relationship. The behaviour of connections has been experimentally and analytically investigated by many researchers (Kishi and Chen 1990, Barsan and Chiorean 1999, Kukreti and Abolmaali 1999, Ivanyi 2000, Chan and Chui 2000, Garlock *et al.* 2003, Ozakgul 2006, Liu 2010, Aksoylar *et al.* 2012, Hadianfard 2012). From these numerous experimental results, it has been understood that the moment-rotation relationship is nonlinear over the entire range of loading for almost all types of connections.

In this study, the independent hardening model (Chen *et al.* 1996, Chan and Chui 2000) is used to simulate the nonlinear connection behaviour under dynamic loading. This model is simple and can be easily applicable to all types of connection models designed for steel frames. In this model, the moment-rotation curve under the first cycle of the loading, unloading and reverse loading remains unchanged under the further repetition of loading cycles. The skeleton curve of this model is derived from the three-parameter power model (Kishi and Chen 1990). The three-parameter power model can be formulated as follows

$$M = \frac{R_{ki} \cdot \theta_r}{\left[1 + (\theta_r / \theta_0)^n\right]^{1/n}} \tag{14}$$

where R_{ki} is the initial connection stiffness, θ_0 is the reference plastic rotation corresponding to M_u/R_{ki} value, M_u is ultimate moment capacity of the connection, and n is the shape parameter. When a connection is loaded, then the tangent stiffness R_{kt} of the connection at an arbitrary rotation θ_r is derived by simply differentiating of Eq. (14) as follows

$$R_{kt} = \frac{dM}{d\theta_r} = \frac{R_{ki}}{\left[1 + (\theta_r / \theta_0)^n\right]^{1+1/n}} \tag{15}$$

Three-parameter power model contains three parameters: initial connection stiffness R_{ki}, ultimate connection moment capacity M_u and shape parameter n. To determine these parameters for a given connection type, practical procedures proposed by Kishi and Chen (1990) are used.

In this study, connections are simulated by rotational springs at the beam ends. Spring element used for a connection is assumed to be massless and dimensionless in size. The R_{xi}, R_{yi}, R_{xj} and R_{yj} are tangent stiffness values of the connections at the i and j ends of the beam-column element in the x and y directions, respectively. Their values are calculated by using the independent hardening model. Herein, as a semi-rigid connection type, top and seat angles with double web-angle connection (TSDWA) is considered.

The element tangent stiffness matrix given by Eq. (3) is then modified to consider the effect of semi-rigid connections for a beam-column element as follows

$$S_1 = \begin{cases} \dfrac{1}{4}\dfrac{((\alpha L)Sin(\alpha L) - (\alpha L)^2 Cos(\alpha L))R_{xi}R_{xj} + (\alpha L)PL \cdot Sin(\alpha L) \cdot R_{xi}}{R_{xi}R_{xj}H_3 + \alpha EI_x H_4(R_{xi} + R_{xj}) + \alpha EI_x PL \cdot Sin(\alpha L)} & if\ P < 0 \\ \dfrac{1}{4}\dfrac{(-(\alpha L)Sinh(\alpha L) + (\alpha L)^2 Cosh(\alpha L))R_{xi}R_{xj} + (\alpha L)PL \cdot Sinh(\alpha L) \cdot R_{xi}}{R_{xi}R_{xj}H_5 + \alpha EI_x H_6(R_{xi} + R_{xj}) + \alpha EI_x PL \cdot Sinh(\alpha L)} & if\ P > 0 \end{cases} \tag{16}$$

$$S_2 = \begin{cases} \dfrac{1}{2}\dfrac{(\alpha L)R_{xi}R_{xj}((\alpha L)-Sin(\alpha L))}{R_{xi}R_{xj}H_3+\alpha EI_x H_4(R_{xi}+R_{xj})+\alpha EI_x PL\cdot Sin(\alpha L)} & if\ P<0 \\ \dfrac{1}{2}\dfrac{(\alpha L)R_{xi}R_{xj}(-(\alpha L)+Sinh(\alpha L))}{R_{xi}R_{xj}H_5+\alpha EI_x H_6(R_{xi}+R_{xj})+\alpha EI_x PL\cdot Sinh(\alpha L)} & if\ P>0 \end{cases} \tag{17}$$

$$S_3 = \begin{cases} \dfrac{1}{4}\dfrac{((\alpha L)Sin(\alpha L)-(\alpha L)^2 Cos(\alpha L))R_{xi}R_{xj}+(\alpha L)PL\cdot Sin(\alpha L)\cdot R_{xj}}{R_{xi}R_{xj}H_3+\alpha EI_x H_4(R_{xi}+R_{xj})+\alpha EI_x PL\cdot Sin(\alpha L)} & if\ P<0 \\ \dfrac{1}{4}\dfrac{(-(\alpha L)Sinh(\alpha L)+(\alpha L)^2 Cosh(\alpha L))R_{xi}R_{xj}+(\alpha L)PL\cdot Sinh(\alpha L)\cdot R_{xj}}{R_{xi}R_{xj}H_5+\alpha EI_x H_6(R_{xi}+R_{xj})+\alpha EI_x PL\cdot Sinh(\alpha L)} & if\ P>0 \end{cases} \tag{18}$$

$$S_4 = \begin{cases} \dfrac{1}{4}\dfrac{((\beta L)Sin(\beta L)-(\beta L)^2 Cos(\beta L))R_{yi}R_{yj}+(\beta L)PL\cdot Sin(\beta L)\cdot R_{yi}}{R_{yi}R_{yj}H_7+\beta EI_y H_8(R_{yi}+R_{yj})+\beta EI_y PL\cdot Sin(\beta L)} & if\ P<0 \\ \dfrac{1}{4}\dfrac{(-(\beta L)Sinh(\beta L)+(\beta L)^2 Cosh(\beta L))R_{yi}R_{yj}+(\beta L)PL\cdot Sinh(\beta L)\cdot R_{yi}}{R_{yi}R_{yj}H_9+\beta EI_y H_{10}(R_{yi}+R_{yj})+\beta EI_y PL\cdot Sinh(\beta L)} & if\ P>0 \end{cases} \tag{19}$$

$$S_5 = \begin{cases} \dfrac{1}{2}\dfrac{(\beta L)R_{yi}R_{yj}((\beta L)-Sin(\beta L))}{R_{yi}R_{yj}H_7+\beta EI_y H_8(R_{yi}+R_{yj})+\beta EI_y PL\cdot Sin(\beta L)} & if\ P<0 \\ \dfrac{1}{2}\dfrac{(\beta L)R_{yi}R_{yj}(-(\beta L)+Sinh(\beta L))}{R_{yi}R_{yj}H_9+\beta EI_y H_{10}(R_{yi}+R_{yj})+\beta EI_y PL\cdot Sinh(\beta L)} & if\ P>0 \end{cases} \tag{20}$$

$$S_6 = \begin{cases} \dfrac{1}{4}\dfrac{((\beta L)Sin(\beta L)-(\beta L)^2 Cos(\beta L))R_{yi}R_{yj}+(\beta L)PL\cdot Sin(\beta L)\cdot R_{yj}}{R_{yi}R_{yj}H_7+\beta EI_y H_8(R_{yi}+R_{yj})+\beta EI_y PL\cdot Sin(\beta L)} & if\ P<0 \\ \dfrac{1}{4}\dfrac{(-(\beta L)Sinh(\beta L)+(\beta L)^2 Cosh(\beta L))R_{yi}R_{yj}+(\beta L)PL\cdot Sinh(\beta L)\cdot R_{yj}}{R_{yi}R_{yj}H_9+\beta EI_y H_{10}(R_{yi}+R_{yj})+\beta EI_y PL\cdot Sinh(\beta L)} & if\ P>0 \end{cases} \tag{21}$$

in which

$$H_3 = 2-2Cos(\alpha L)-(\alpha L)Sin(\alpha L) \tag{22}$$

$$H_4 = Sin(\alpha L)-(\alpha L)Cos(\alpha L) \tag{23}$$

$$H_5 = 2-2Cosh(\alpha L)+(\alpha L)Sinh(\alpha L) \tag{24}$$

$$H_6 = -Sinh(\alpha L)+(\alpha L)Cosh(\alpha L) \tag{25}$$

$$H_7 = 2-2Cos(\beta L)-(\beta L)Sin(\beta L) \tag{26}$$

$$H_8 = Sin(\beta L)-(\beta L)Cos(\beta L) \tag{27}$$

$$H_9 = 2-2Cosh(\beta L)+(\beta L)Sinh(\beta L) \tag{28}$$

$$H_{10} = -Sinh(\beta L)+(\beta L)Cosh(\beta L) \tag{29}$$

3. Numerical procedures

The equation of motion for frames subjected to dynamic actions can be given by

$$M \cdot \Delta\ddot{x} + C \cdot \Delta\dot{x} + K \cdot \Delta x = \Delta P \tag{30}$$

in which K is the stiffness matrix (the tangent stiffness matrix + the geometric stiffness matrix) for the system of structural elements; M is the mass matrix; $C=\alpha M+\beta K_i$ is the viscous damping matrix, where α and β are damping factors proportional to mass and stiffness, respectively, and K_i is the initial stiffness matrix; $\Delta\ddot{x}$, $\Delta\dot{x}$, Δx and ΔP are incremental acceleration, velocity, displacement and externally applied force vectors for the time step size Δt, respectively.

For any time step choosen, the equation of motion is integrated by using a step-by-step integration method based on assumption of constant acceleration (Chopra 2012). In this method, the velocity and displacement vectors are calculated as follows

$$\dot{x}_{t+\Delta t} = \dot{x}_t + (1-\delta_1)\Delta t\ddot{x}_t + \delta_1 \Delta t \ddot{x}_{t+\Delta t} \tag{31}$$

$$x_{t+\Delta t} = x_t + \Delta t\dot{x}_t + \left(\frac{1}{2} - \delta_2\right)\Delta t^2 \ddot{x}_t + \delta_2 \Delta t^2 \ddot{x}_{t+\Delta t} \tag{32}$$

where x_t, $\dot{x}_t$ and $\ddot{x}_t$ are the total displacement, velocity and acceleration vectors for the time t; δ_1 and δ_2 parameters are 1/2 and 1/4, respectively.

Eqs. (31) and (32) can be rewritten for the incremental displacements in the following form

$$\Delta\dot{x} = \frac{\delta_1}{\delta_2 \Delta t}\Delta x - \frac{\delta_1}{\delta_2}\Delta t\dot{x}_t + \left(1 - \frac{\delta_1}{2\delta_2}\right)\Delta t\ddot{x}_t \tag{33}$$

$$\Delta\ddot{x} = \frac{1}{\delta_2 \Delta t^2}\Delta x - \frac{1}{\delta_2 \Delta t}\dot{x}_t - \frac{1}{2\delta_2}\ddot{x}_t \tag{34}$$

By substituting Eqs. (33) and (34) into the Eq. (30), the dynamic equilibrium of the space frame system in terms of the unknown incremental nodal displacement Δx can be expressed as follows

$$\left[K + \frac{1}{\delta_2 \Delta t^2}M + \frac{\delta_1}{\delta_2 \Delta t}C\right]\Delta x = \Delta P + \left[\frac{1}{\delta_2 \Delta t}M + \frac{\delta_1}{\delta_2}C\right]\dot{x}_t + \left[\frac{1}{2\delta_2}M + \Delta t(\frac{\delta_1}{2\delta_2} - 1)C\right]\ddot{x}_t \tag{35}$$

When the incremental displacement Δx for the next time step $t+\Delta t$ in Eq. (35) is solved, then the acceleration, velocity, displacement and force vectors can be updated by using the following equations

$$x_{t+\Delta t} = x_t + \Delta x \tag{36}$$

$$\dot{x}_{t+\Delta t} = \dot{x}_t + \Delta\dot{x} \tag{37}$$

$$\ddot{x}_{t+\Delta t} = \ddot{x}_t + \Delta\ddot{x} \tag{38}$$

$$P_{t+\Delta t} = P_t + \Delta P \tag{39}$$

For the next time steps, this solution is repeated from Eq. (33) until a structural failure i.e. a numerical instability occurrence or the end of the time duration.

4. Evaluation of energy response

The energy response i.e., the variation of the energy within the time is performed by using the energy formulations obtained from the integration of the equation of motion in the time domain. The seismic input energy imparted to the structure that is subjected to earthquake ground motion is equal to the sum of recoverable elastic strain energy, dissipated energy due to the nonlinear behavior at each plactic hinge and connection, damping and kinetic energies so that the equilibrium equation for the total energy can be written as (Zahrah and Hall 1984, Uang and Bertero 1990, Leger and Dassault 1992, Salazar and Haldar 2001, Wong and Yang 2002, Sekulovic and Nefovska-Danilovic 2008, Wang and Wong 2009)

$$E_i(t) = E_e(t) + E_d(t) + E_{dis}(t) + E_k(t) \tag{40}$$

where $E_i(t)$ is the seismic input energy, $E_e(t)$ is the elastic strain energy, $E_d(t)$ is the damping energy, $E_{dis}(t)$ is the dissipated energy, and $E_k(t)$ is the kinetic energy.

Each energy component can be evaluated as (Wong and Yang 2002, Sekulovic and Nefovska-Danilovic 2008, Wang and Wong 2009)

$$E_i(t) = -\int_0^t \dot{x}^T M \ II \ \ddot{x}_g \, dt \tag{41}$$

$$E_e(t) = \frac{1}{2} \dot{x}_e^T K_e x_e \tag{42}$$

$$E_d(t) = \int_0^t \dot{x}^T C \ \dot{x} \ dt \tag{43}$$

$$E_{dis}(t) = \int_0^t \dot{x}^T K \ x \ dt - E_e(t) \tag{44}$$

$$E_k(t) = \frac{1}{2} \dot{x}^T M \ \dot{x} \tag{45}$$

where K_e and x_e are the elastic stiffness matrix and elastic displacement vector, respectively, $\ddot{x}_g$ is the ground acceleration, x and $\dot{x}$ are the total displacement and velocity vectors at time t, respectively, where II is the matrix that matches the earthquake acceleration components to the corresponding nodal degrees of freedom.

Finally, for the proposed analysis procedure, the error analysis is also carried out by calculating the relative error from the energy balance at the arbitrary time t (Austin and Lin 2004). Thus, the accuracy and suitability of the numerical evaluation performed herein are checked as follows

$$Relative\ error\ (\%) = \frac{E_i(t) - E_e(t) - E_d(t) - E_{dis}(t) - E_k(t)}{E_i(t)} \times 100 \tag{46}$$

Additionally, the error time history, i.e., the variation of error versus time during any earthquake excitation is easily obtained as well as graphically shown.

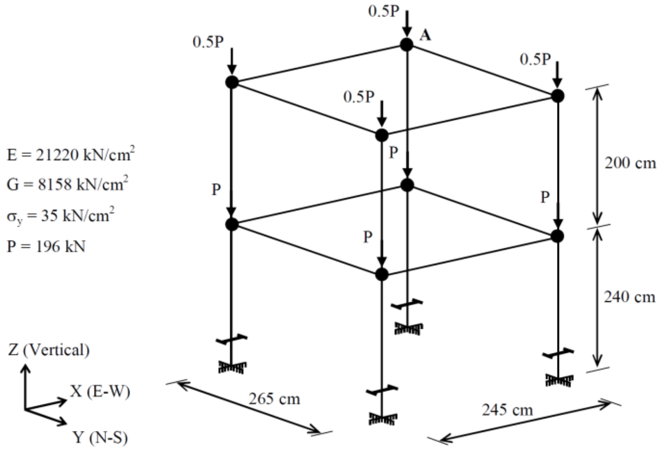

Fig. 2 Two-storey one-bay space frame (Kim *et al.* 2006)

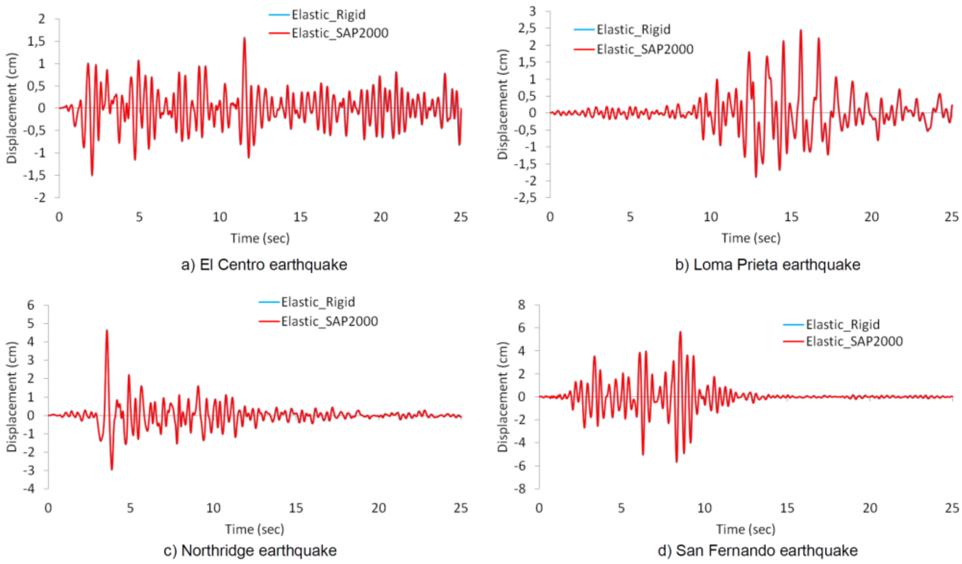

Fig. 3 Elastic displacement responses (x_A) of a two-storey space frame

5. Numerical studies

For the numerical examples, three-dimensional steel frames presented by Kim *et al.* (2006) are used. As the ground motion input data, El Centro 1940 (station: Imperial Valley), San Fernando 1971 (station: Pacoima Dam), Loma Prieta 1989 (station: Emeryville) and Northridge 1994 (station: 0637 Sepulveda VA) earthquake records with three components are used (USGS, 2014). Damping factors proportional to mass and stiffness are chosen as corresponding to 5% viscous damping ratio. As the semi-rigid beam-to-column connection type, a top and seat angle with double web angle (TSDWA) type of connection is used. The tangent stiffness, ultimate moment capacity and shape parameter for the connections are calculated by using the procedure proposed

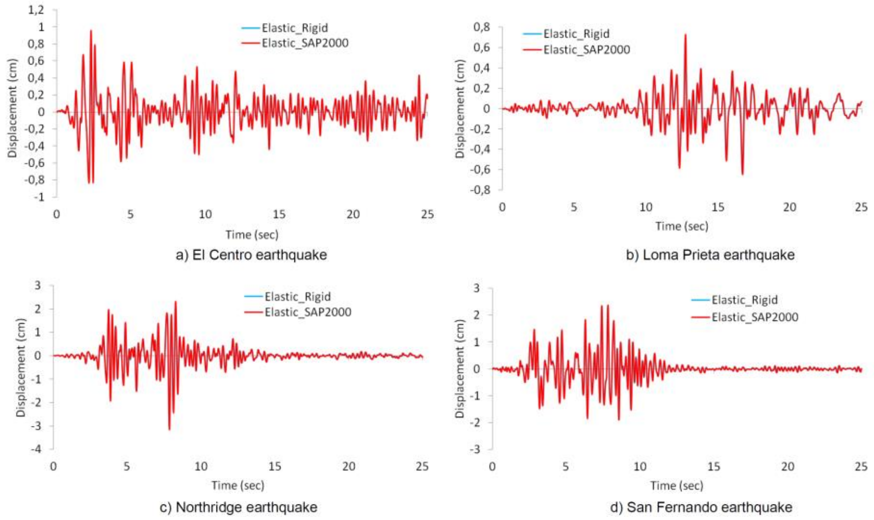

Fig. 4 Elastic displacement responses (y_A) of a two-storey space frame

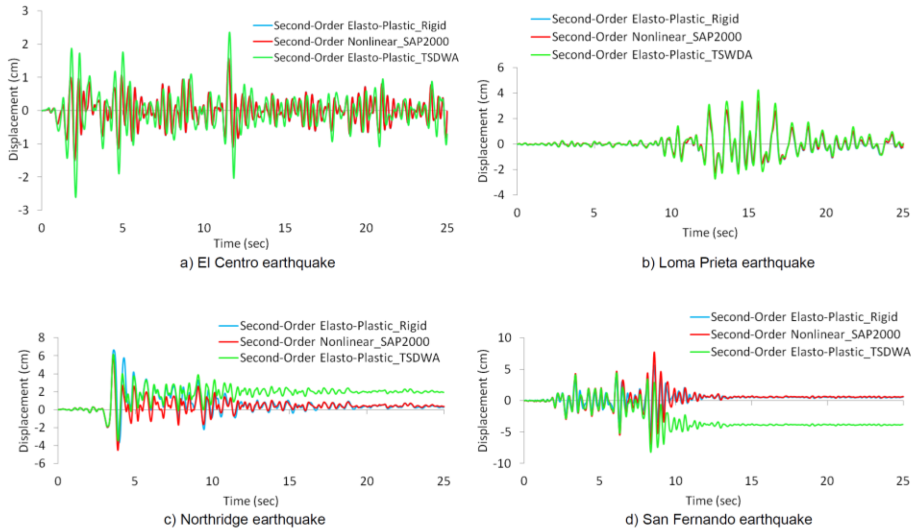

Fig. 5 Nonlinear displacement responses (x_A) of a two-storey space frame

by Kishi and Chen (1990). Each member of considered space frames is modeled by one element only.

5.1 Two-storey one-bay space frame

The geometric properties and other pertinent information of the space frame with lumped masses at the nodes are given in Fig. 2. All sections are composed of H125×125×6.5×9.

Then the results obtained from the linear and nonlinear time-history analysis are compared with the values calculated by the commercial finite element analysis software SAP2000 (2011) in order

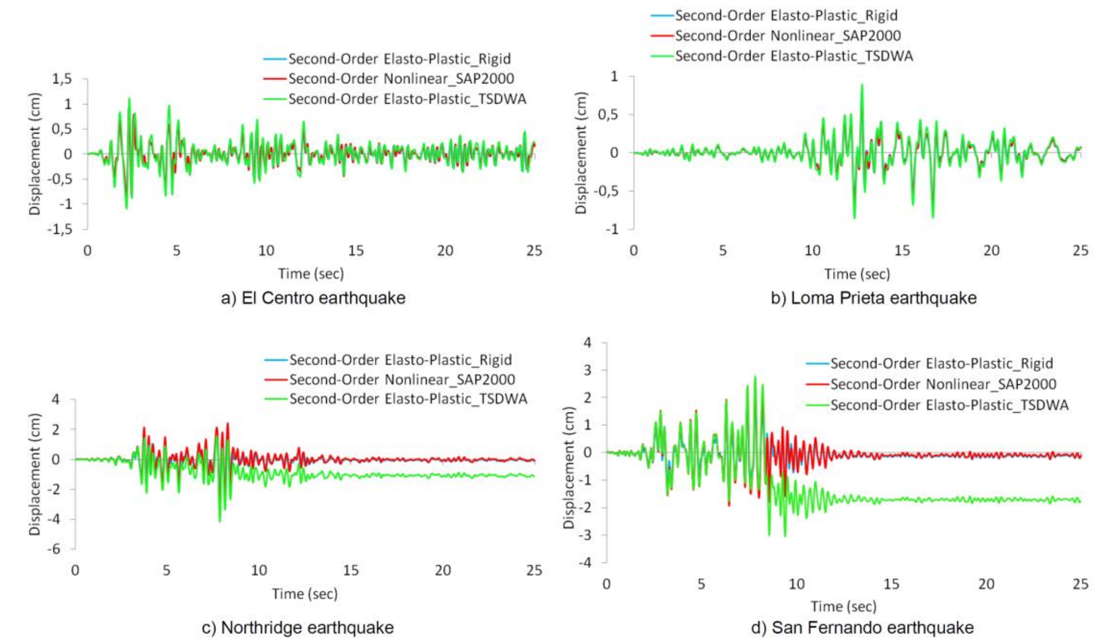

Fig. 6 Nonlinear displacement responses (y_A) of a two-storey space frame

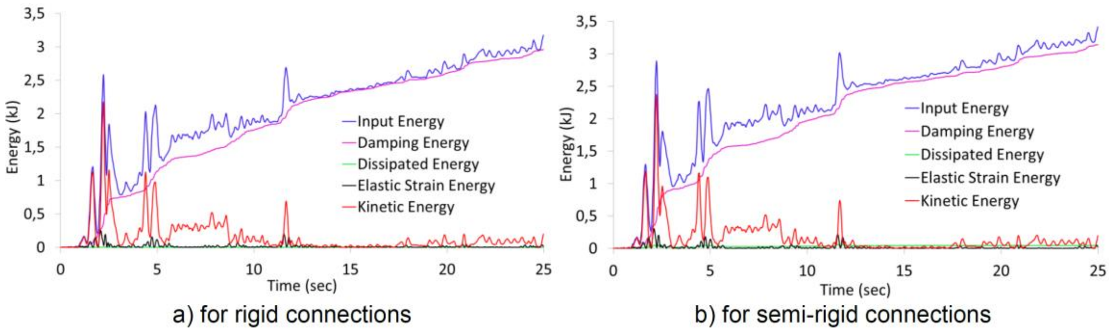

Fig. 7 Energy response of a two-storey space frame subjected to El Centro earthquake

to check the accuracy and capability of the proposed analysis method. It can be seen that the results obtained from the proposed analysis method as well as by using SAP2000 (2011) are exactly equivalent to the elastic analysis, and approximately identical to the inelastic time-history analysis.

The displacement responses along *x*-axis and *y*-axis for the node *A* of the space frame with rigid connections according to the linear analysis are shown in Figs. 3 and 4, respectively.

The nonlinear responses along *x*-axis and *y*-axis for the node *A* of the rigid and semi-rigid space frames are shown in Figs. 5 and 6, respectively.

In case of a comparison based on the computational efficiency, it is found out that the proposed analysis method has much higher efficiency than the analysis carried out by SAP2000 (2011). For example, in the nonlinear time-history analysis for the San Fernando earthquake, the solution time of the proposed analysis is recorded about 20 seconds, while quite a lot time, i.e. approximately 10 minutes are needed for the SAP2000 (2011) analysis.

According to the results obtained from the nonlinear analysis of the Northridge and San Fernando earthquakes (see Figs. 5 and 6), it can be seen that plastic hinges i.e. permanent deformations occur on this space frame.

After the proposed analysis results are accurately compared with SAP2000 (2011) results, the energy response analysis of rigid and semi-rigid frames are carried out and the time-history curves obtained for each energy form are plotted in Figs. 7-10. Using these curves, it can be seen that how the energy varies with time during the earthquake excitations.

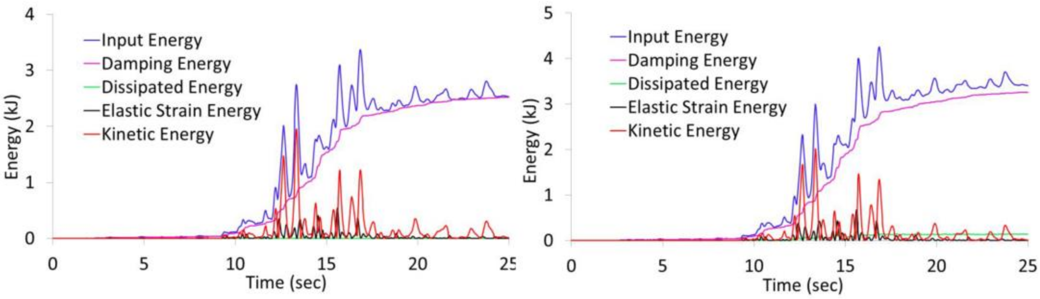

a) for rigid connections b) for semi-rigid connections

Fig. 8 Energy response of a two-storey space frame subjected to Loma Prieta earthquake

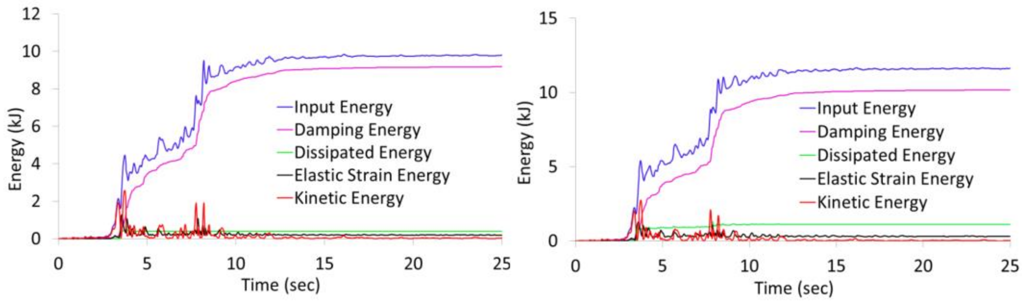

a) for rigid connections b) for semi-rigid connections

Fig. 9 Energy response of a two-storey space frame subjected to Northridge earthquake

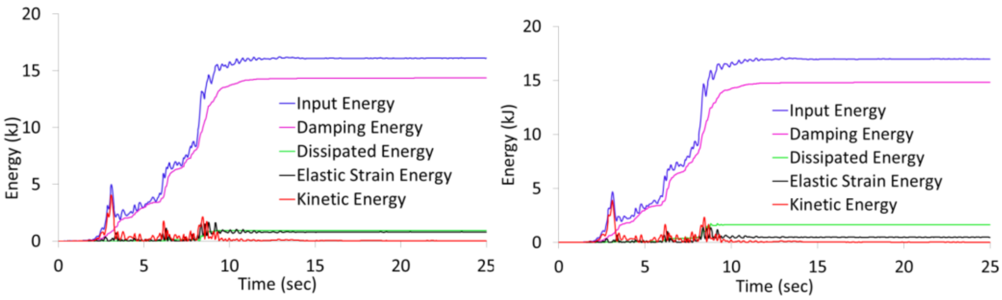

a) for rigid connections b) for semi-rigid connections

Fig. 10 Energy response of a two-storey space frame subjected to San Fernando earthquake

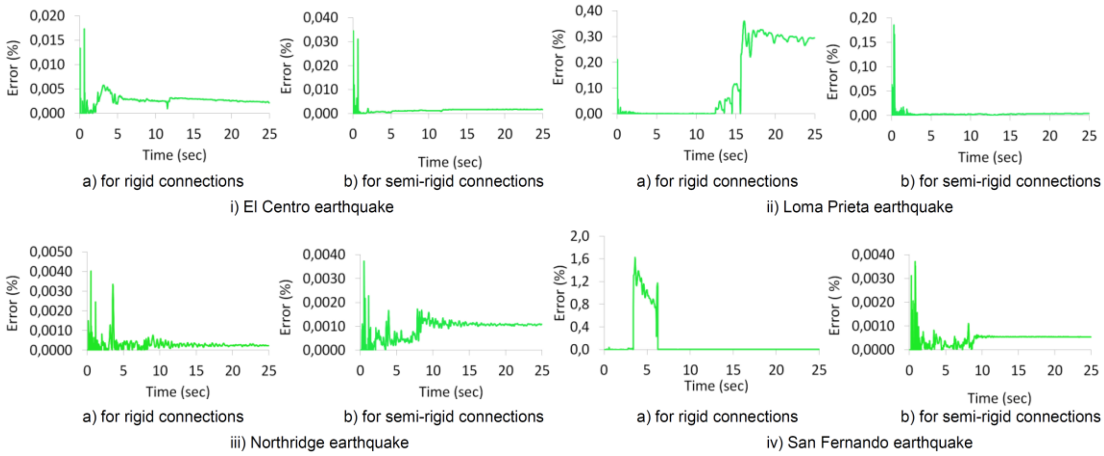

Fig. 11 Error time-history curves of a two-storey space frame

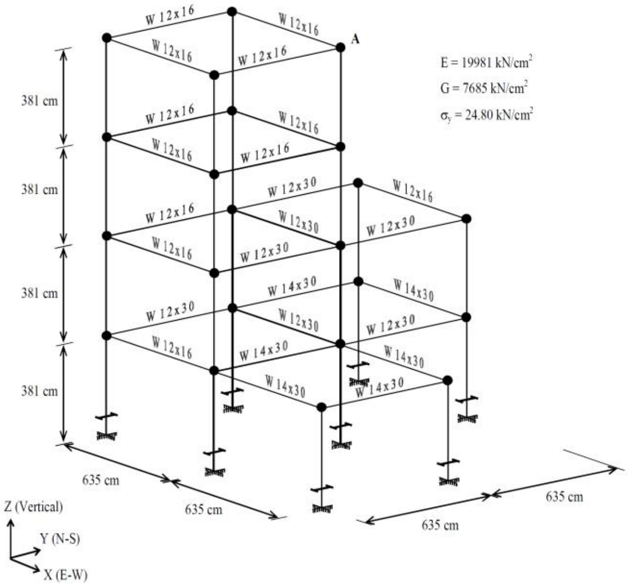

Fig. 12 Four-storey two-bay space frame (Kim *et al.* 2006)

To quantify the accuracy of the proposed nonlinear solution procedure, the error analysis based on Eq. (46) is performed so that the relative error as well as its variations versus time is obtained for each excitation or ground motion as plotted in Fig. 11.

As can be seen in Fig. 11, the maximum percentage of the relative error is about 1.6%. It can be seen that this value shows high accuracy for the nonlinear analysis procedure proposed herein.

5.2 Four-storey two-bay space frame

The geometric properties and other pertinent information of the steel frame with lumped masses at the nodes are given in Fig. 12.

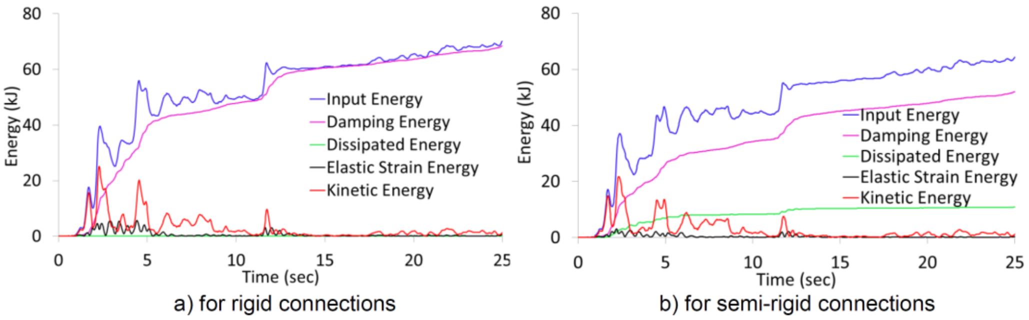

Fig. 13 Energy response of a four-storey space frame subjected to El Centro earthquake

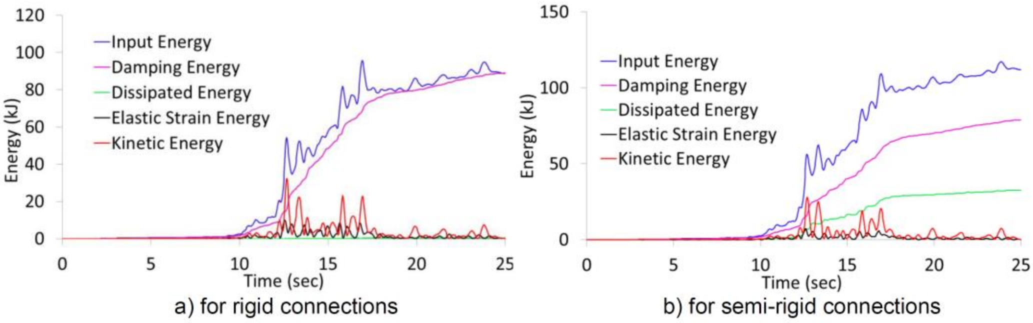

Fig. 14 Energy response of a four-storey space frame subjected to Loma Prieta earthquake

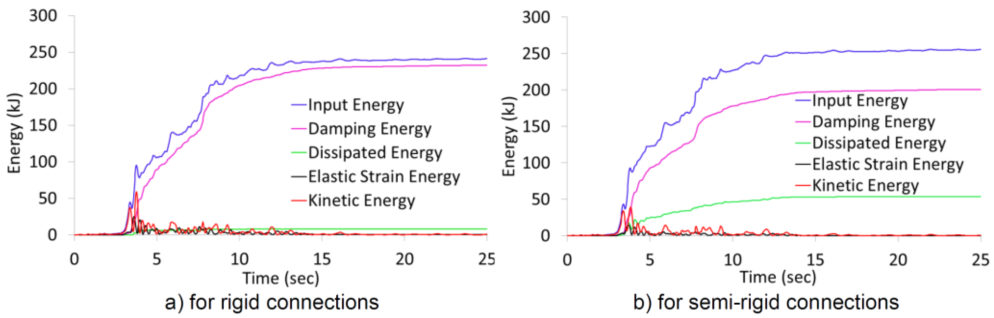

Fig. 15 Energy response of a four-storey space frame subjected to Northridge earthquake

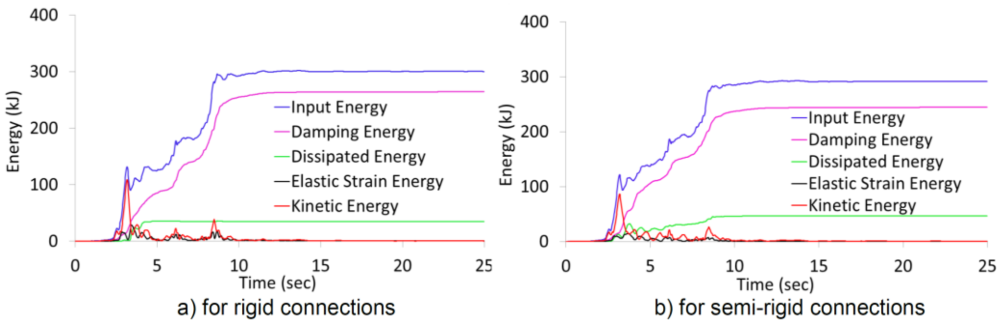

Fig. 16 Energy response of a four-storey space frame subjected to San Fernando earthquake

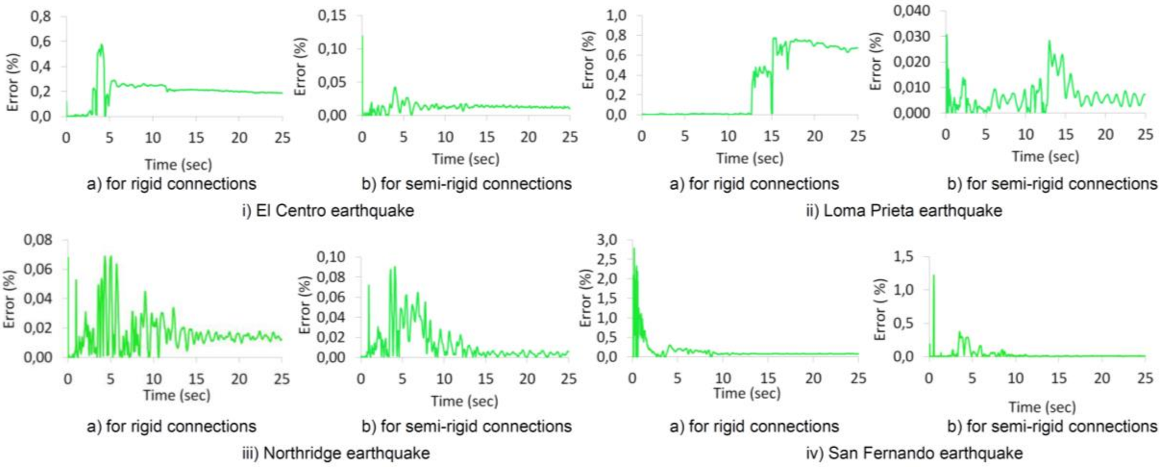

Fig. 17 Error time-history curves of a four-storey space frame

As abovementioned, the linear and nonlinear time-history analysis for this steel space frame are carried out. Hence the energy responses obtained for various ground motions are shown in Figs. 13-16.

For each nonlinear analysis, the needed relative error versus time is obtained from the error analysis, and the variation of error in time domain is plotted in Fig. 17. Based on these analysis results, it can be seen that the maximum percentage of the relative error is approximately 2.8%.

6. Conclusions

In this study, a very accurate and efficient evaluation for inelastic space frames subjected to significant earthquake ground motions is aimed. For this purpose, the nonlinear behavior of steel frames is firstly defined by using an algorithm considering the nonlinearities for material, geometry and different types of connections. Then, the energy response analysis based on this method and seismic energy formulations is performed under various significant earthquake excitations experienced. The seismic input energy imparted to the space frame structure and its components having various energy forms such as damping energy, dissipated energy, strain energy and kinetic energy versus time are calculated. The accuracy of the obtained results is controlled by calculating the relative error based on the energy balance concept. So it can be seen that the relative error obtained and plotted for a given time history of any earthquake varies within the time duration. For example from the error time history of San Fernando earthquake max. relative error value is calculated as approximately 2.8% in this study. Thus, unlike previous studies, for the first time, the error time-history response is obtained from the nonlinear analysis of space frames, and the corresponding error curves are also plotted.

Based on the energy time-history responses, it can be seen that each energy form such as input energy, elastic strain energy, damping energy, dissipated energy and kinetic energy is approximately zero at the beginning of any earthquake ground excitation. However, with time the input energy in the structure is increasing. At the moments where the earthquake excitation reaches its maximum values, bounces for the input energy appear, and high increase can be especially observed for the kinetic energy. Towards the end of the excitation, while the input energy generally approximates to a stable constant value, which mainly equals to the sum of the damping and dissipated energy, the kinetic energy as well as the elastic strain energy which are temporarily stored in the structure during the ground motions are approximately equal to zero. In the case of the El Centro and Loma Prieta earthquakes, the results demonstrate that the nonlinear responses of the structures remain in elastic range and, thereby no full plastic hinges form, and no irrecoverable hysteretic energy due to plastic deformations occurs, in consequence the input energy is nearly equal to the sum of the damping and kinetic energies. According to the results obtained from the proposed analysis, it can be seen that the energy, linear and nonlinear displacement responses versus time of rigid and semi-rigid frames are meaningfully different. Even though the elasto-plastic rotations in the rigid frames are larger than the hysteretic rotations of the connections in the semi-rigid frames having a nonlinear behavior, it is seen that the energy dissipated by hysteretic behaviour of the connections can be greater than the value of the corresponding energy form occurred in the rigid frames. Additionally, it can be seen that the damping energy is the major response parameter for both rigid and semi-rigid frames.

References

Aksoylar, N.D., Elnashai, A.S. and Mahmoud, H. (2012), “Seismic performance of semirigid moment-resisting frames under far and near field records”, *ASCE J. Struct. Eng.*, **138**(2), 157-169.

Austin, M.A. and Lin, W.J. (2004), “Energy balance assessment of base-isolated structures”, *ASCE J. Struct. Eng.*, **130**(3), 347-358.

Barsan, G.M. and Chiorean, C.G. (1999), “Computer program for large deflection elasto-plastic analysis of semi-rigid steel frameworks”, *Comput. Struct.*, **72**(6), 699-711.

Chan, S.L. and Chui, P.P.T. (2000), *Non-linear static and cyclic analysis of steel frames with semi-rigid connections*, Elsevier Science Publishing Co., New York, NY, USA.

Chan, S.L. and Zhou, Z.H. (1995), “Second-order elastic analysis of frames using single imperfect element per member”, *ASCE J. Struct. Eng.*, **121**(6), 939-945.

Chen, W.F. and Chan, S.L. (1995), “Second-order inelastic analysis of steel frames using element with midspan and end springs”, *ASCE J. Struct. Eng.*, **121**(3), 530-541.

Chen, W.F., Goto, Y. and Liew, J.Y.R. (1996), *Stability design of semi-rigid frames*, John Wiley & Sons Inc., New York, NY, USA.

Chiorean, C.G. (2009), “A computer method for nonlinear inelastic analysis of 3D semi-rigid steel frameworks”, *Eng. Struct.*, **31**(12), 3016-3033.

Chiorean, C.G. and Barsan, G.M. (2005), “Large deflection distributed plasticity analysis of 3D steel frameworks”, *Comput. Struct.*, **83**(19-20), 1555-1571.

Chopra, A.K. (2012), *Dynamics of structures: theory and applications to earthquake engineering*, Prentice-Hall, New Jersey, NJ, USA.

Ekhande, S.G., Selvappalam, M. and Madugula, M.K.S. (1989), “Stability functions for three-dimensional beam-columns”, *ASCE J. Struct. Div.*, **115**(2), 467-479.

Garlock, M.M., Ricles, J.M. and Sause, R. (2003), “Cyclic load tests and analysis of bolted top-and-seat angle connections”, *ASCE J. Struct. Eng.*, **129**(12), 1615-1625.

Gong, Y., Xue, Y., Xu, L. and Grierson, D.E. (2012), “Energy-based design optimization of steel building frameworks using nonlinear response history analysis”, *J. Construct. Steel Res.*, **68**(1), 43-50.

Hadianfard, M.A. (2012), “Using integrated displacement method to time-history analysis of steel frames with nonlinear flexible connections”, *Struct. Eng. Mech.*, **41**(5), 675-689.

Ivanyi, M. (2000), “Full-scale tests of steel frames with semi-rigid connections”, *Eng. Struct.*, **22**(2), 168-179.

Jonatowski, J.J. and Birnstiel, C. (1970), "Inelastic stiffened suspension space structures", *ASCE J. Struct. Div.*, **96**(6), 1143-1166.

Kalkan, E. and Kunnath, S.K. (2008), "Relevance of absolute and relative energy content in seismic evaluation of structures", *Adv. Struct. Eng.*, **11**(1), 1-18.

Kim, S.E., Ngo-Huu, C. and Lee, D.H. (2006), "Second-order inelastic dynamic analysis of 3-D steel frames", *Int. J. Solid. Struct.*, **43**(6), 1693-1709.

Kim, S.E., Park, M.H. and Choi, S.H. (2001), "Direct design of three-dimensional frames using practical advanced analysis", *Eng. Struct.*, **23**(11), 1491-1502.

Kishi, N. and Chen, W.F. (1990), "Moment-rotation relations of semi-rigid connections with angles", *ASCE J. Struct. Eng*., **116**(7), 1813-1834.

Kukreti, A.R. and Abolmaali, A.S. (1999), "Moment-rotation hysteresis behavior of top and seat angle steel frame connections", *ASCE J. Struct. Eng*., **125**(8), 810-820.

Leger, P. and Dussault, S. (1992), "Seismic-energy dissipation in MDOF structures", *ASCE J. Struct. Eng*., **118**(5), 1251-1269.

Liew, J.Y.R., Chen, H., Shanmugam, N.E. and Chen, W.F. (2000), "Improved nonlinear plastic hinge analysis of space frame structures", *Eng. Struct.*, **22**(10), 1324-1338.

Liu, Y. (2010), "Semi-rigid connection modeling for steel frameworks", *Struct. Eng. Mech.*, **35**(4), 431-457.

Manfredi, G. (2001), "Evaluation of seismic energy demand", *Earthq. Eng. Struct. Dyn.*, **30**(4), 485-499.

Moustafa, A. (2011), "Damage-based design earthquake loads for single-degree-of-freedom inelastic structures", *ASCE J. Struct. Eng*., **137**(3), 456-467.

Ngo-Huu, C., Kim, S.E. and Oh, J.R. (2007), "Nonlinear analysis of space steel frames using fiber plastic hinge concept", *Eng. Struct.*, **29**(4), 649-657.

Ngo-Huu, C., Nguyen, P.C. and Kim, S.E. (2012), "Second-order plastic-hinge analysis of space semi-rigid steel frames", *Thin Wall. Struct.*, **60**, 98-104.

Nguyen, P.C. and Kim, S.E. (2013), "Nonlinear elastic dynamic analysis of space steel frames with semi-rigid connections", *J. Construct. Steel Res.*, **84**, 72-81.

Orbison, J.G., McGuire, W. and Abel, J.F. (1982), "Yield surface applications in nonlinear steel frame analysis", *Comput. Meth. Appl. Mech. Eng.*, **33**(1-3), 557-573.

Ozakgul, K. (2006), "Determination of failure mechanisms and ductility of 3D steel frames under earthquake loads with three components", PhD Dissertation, Istanbul Technical University, Istanbul.

Salazar, A.R. and Haldar, A. (2001), "Energy dissipation at PR frames under seismic loading", *ASCE J. Struct. Eng*., **127**(5), 588-592.

SAP2000, (2011), *Structural analysis program*, Computers and Structures Inc., Berkeley, California, USA.

Segal, F. and Val, D.V. (2006), "Energy evaluation for Ramberg-Osgood hysteretic model", *ASCE J. Struct. Eng*., **132**(9), 907-913.

Sekulovic, M. and Nefovska-Danilovic, M. (2008), "Contribution to transient analysis of inelastic steel frames with semi-rigid connections", *Eng. Struct.*, **30**(4), 976-989.

Shugyo, M. (2003), "Elastoplastic large deflection analysis of three-dimensional steel frames", *ASCE J. Struct. Eng*., **129**(9), 1259-1267.

Thai, H.T. and Kim, S.E. (2011), "Second-order inelastic dynamic analysis of steel frames using fiber hinge method", *J. Construct. Steel Res.*, **67**(10), 1485-1494.

Uang, C.M. and Bertero, V.V. (1990), "Evaluation of seismic energy in structures", *Earthq. Eng. Struct. Dyn.*, **19**(1), 77-90.

USGS, (2014), United State Geological Survey, National Strong-Motion Project, http://nsmp.wr.usgs.gov.

Uzgider, E.A. (1980), "Inelastic response of space frames to dynamic loads", *Comput. Struct.*, **11**(1-2), 97-112.

Wang, Z. and Wong, K.K.F. (2009), "Energy evaluation of inelastic structures subjected to random earthquake excitations", *Struct. Des. Tall Spec. Build.*, **18**(5), 559-571.

White, D.W., Surovek, A.E., Alemdar, B.N., Chang, C.J., Kim, Y.D. and Kuchenbecker, G.H. (2006), "Stability analysis and design of steel building frames using the 2005 AISC specification", *Steel Struct.*, **6**, 71-91.

Wong, K.K.F. and Wang, Y. (2001), "Energy-based damage assessment on structures during earthquakes", *Struct. Des. Tall Spec. Build.*, **10**(2), 135-154.

Wong, K.K.F. and Yang, R. (2002), "Earthquake response and energy evaluation of inelastic structures", *ASCE J. Eng. Mech.*, **128**(3), 308-317.

Wong, K.K.F. and Zhao, D. (2007), "Uncoupling of potential energy in nonlinear seismic analysis of framed structures", *ASCE J. Eng. Mech.*, **133**(10), 1061-1071.

Zahrah, T.F. and Hall, W.J. (1994), "Earthquake energy absorption in SDOF structures", *ASCE J. Eng. Mech.*, **110**(8), 1757-1772.

CC